Phytophthora sojae effector Avr1d functions as an E2 competitor and inhibits ubiquitination activity of GmPUB13 to facilitate infection

Yachun Lin[a,b,c,1], Qinli Hu[d,e,1], Jia Zhou[d,e], Weixiao Yin[a,f], Deqiang Yao[g], Yuanyuan Shao[a], Yao Zhao[a,b,c], Baodian Guo[a,b,c], Yeqiang Xia[a,b,c], Qian Chen[h,i], Yan Wang[a,b,c], Wenwu Ye[a,b,c], Qi Xie[i], Brett M. Tyler[j], Weiman Xing[k,2], and Yuanchao Wang[a,b,c,2]

[a]Department of Plant Pathology, Nanjing Agricultural University, 210095 Nanjing, China; [b]The Key Laboratory of Integrated Management of Crop Diseases and Pests (Ministry of Education), Nanjing Agricultural University, 210095 Nanjing, China; [c]The Key Laboratory of Plant Immunity, Nanjing Agricultural University, 210095 Nanjing, China; [d]Shanghai Center for Plant Stress Biology and Center of Excellence in Molecular Plant Sciences, Chinese Academy of Sciences, Shanghai 200032, China; [e]University of Chinese Academy of Sciences, Beijing 100049, China; [f]Department of Plant Pathology, College of Plant Science and Technology and the Key Lab of Crop Disease Monitoring and Safety Control in Hubei Province, Huazhong Agricultural University, 430070 Wuhan, China; [g]iHuman Institute, ShanghaiTech University, Shanghai 201210, China; [h]Ministry of Agriculture Key Lab of Pest Monitoring and Green Management, Department of Plant Pathology, College of Plant Protection, China Agricultural University, 100193 Beijing, China; [i]State Key Laboratory of Plant Genomics, Institute of Genetics and Developmental Biology, The Innovative Academy of Seed Design, Chinese Academy of Sciences, Beijing 100101, China; [j]Center for Genome Research and Biocomputing, Department of Botany and Plant Pathology, Oregon State University, Corvallis, OR 97331; and [k]Shanghai Key Laboratory of Plant Molecular Sciences, College of Life Sciences, Shanghai Normal University, Shanghai 200234, China

Edited by Sheng Yang He, Duke University, and approved January 29, 2021 (received for review August 31, 2020)

Oomycete pathogens such as *Phytophthora* secrete a repertoire of effectors into host cells to manipulate host immunity and benefit infection. In this study, we found that an RxLR effector, Avr1d, promoted *Phytophthora sojae* infection in soybean hairy roots. Using a yeast two-hybrid screen, we identified the soybean E3 ubiquitin ligase GmPUB13 as a host target for Avr1d. By coimmunoprecipitation (Co-IP), gel infiltration, and isothermal titration calorimetry (ITC) assays, we confirmed that Avr1d interacts with GmPUB13 both in vivo and in vitro. Furthermore, we found that Avr1d inhibits the E3 ligase activity of GmPUB13. The crystal structure Avr1d in complex with GmPUB13 was solved and revealed that Avr1d occupies the binding site for E2 ubiquitin conjugating enzyme on GmPUB13. In line with this, Avr1d competed with E2 ubiquitin conjugating enzymes for GmPUB13 binding in vitro, thereby decreasing the E3 ligase activity of GmPUB13. Meanwhile, we found that inactivation of the ubiquitin ligase activity of GmPUB13 stabilized GmPUB13 by blocking GmPUB13 degradation. Silencing of GmPUB13 in soybean hairy roots decreased *P. sojae* infection, suggesting that GmPUB13 acts as a susceptibility factor. Altogether, this study highlights a virulence mechanism of *Phytophthora* effectors, by which Avr1d competes with E2 for GmPUB13 binding to repress the GmPUB13 E3 ligase activity and thereby stabilizing the susceptibility factor GmPUB13 to facilitate *Phytophthora* infection. This study unravels the structural basis for modulation of host targets by *Phytophthora* effectors and will be instrumental for boosting plant resistance breeding.

effector | U-box | self-ubiquitination | crystal structure | susceptibility factor

In nature, plants are continuously challenged by various microbes. During long-term coevolution, plants have developed innate immune systems to discriminate among microbes by recognizing microbe/pathogen-associated molecular patterns (MAMPs/PAMPs) and microbial effectors, and thereby mounting MAMP/PAMP-triggered immunity (MTI/PTI) responses, respectively. For productive infection, plant pathogens secrete a complex repertoire of effectors to modulate host immunity to favor infection (1).

Ubiquitination has emerged as a crucial posttranslational modification of proteins, as it plays an important role in regulating various cellular processes, including plant immune responses (2, 3). In general, ubiquitination involves addition of ubiquitin to target proteins by sequential actions of an E1 ubiquitin activating enzyme, an E2 ubiquitin conjugating enzyme, and an E3 ubiquitin ligase. Ubiquitination can trigger degradation or may modify the function of the target protein. E3 ubiquitin ligases AtPUB13 and AtPUB12 are well-studied negative regulators of *Arabidopsis thaliana* immunity, which attenuate the immune responses triggered by the bacteria PAMP flg22 (4, 5). AtPUB13 also ubiquitinates the chitin receptor AtLYK5, which is required for AtLYK5 turnover; the mutant *pub13* is more sensitive to chitin treatment (6). The oomycete pathogen *Phytophthora sojae* is the causal agent of root and stem rot of soybean, which accounts for millions of dollars of annual loss worldwide (7). During infection, *P. sojae* secretes a repertoire of effectors with a conserved N-terminal "RxLR" motif into host cells (8). Avr1d (Avh6) is one such effector and previously was identified as an avirulence effector which can be recognized by soybean plants carrying the resistance gene *Rps1d*, triggering ETI (9). In this study, we found that Avr1d was a virulence factor that promotes *P. sojae* infection when overexpressed in soybean hairy

Significance

Ubiquitination acts as a crucial regulator in plant immunity. Accordingly, microbial pathogens secrete effectors to hijack the host ubiquitination system. However, the molecular mechanisms by which effectors modulate the host ubiquitination system are not yet clear. Here, we found that the *Phytophthora sojae* effector Avr1d physically binds to the U-box-type E3 ligase GmPUB13, which proved to be a susceptibility factor. The crystal structure of Avr1d complexed with GmPUB13 revealed that Avr1d occupies the binding site in GmPUB13 for E2 ubiquitin conjugating enzyme and competes with E2 for binding to GmPUB13. Avr1d stabilized GmPUB13 by suppressing the self-ubiquitination activity of GmPUB13 and thereby promoting *Phytophthora* infection. This study reveals a structural basis for modulation of host targets by *Phytophthora* effectors.

Author contributions: Y.L., Q.H., W.X., and Yuanchao Wang designed research; Y.L., Q.H., J.Z., W. Yin, Y.S., and Q.C. performed research; Y.L., Q.H., J.Z., W. Ye., D.Y., Y.S., Y.Z., B.G., Y.X., and Q.C. analyzed data; and Y.L., Q.H., Yan Wang, W. Ye, Q.X., B.M.T., W.X., and Yuanchao Wang wrote the paper.

The authors declare no competing interest.

This article is a PNAS Direct Submission.

[1]Y.L. and Q.H. contributed equally to this work.

[2]To whom correspondence may be addressed. Email: weimanxing@shnu.edu.cn or wangyc@njau.edu.cn.

This article contains supporting information online at https://www.pnas.org/lookup/suppl/doi:10.1073/pnas.2018312118/-/DCSupplemental.

Published March 3, 2021.

roots. During *P. sojae* infection, Avr1d targets two highly homologous U-box ARM-repeats-type E3 ligases in soybean, Glyma12g06860 and Glyma11g14910, which are phylogenetically close to AtPUB13 and were named as GmPUB13 and GmPUB13-like (GmPUB13L), respectively. Silencing GmPUB13 and GmPUB13L in soybean hairy roots increased the resistance to *P. sojae*. Avr1d physically binds to GmPUB13 and blocks the ubiquitin ligase activity of GmPUB13 by competing with E2 ubiquitin conjugating enzyme for the U-box domain. This study reveals the structural basis for modulation of host targets by a *Phytophthora* effector and provides mechanistic insights into the promotion of host susceptibility by *Phytophthora* effectors.

Results

Avr1d Promotes *P. sojae* Infection. To determine whether Avr1d acts as a virulence effector, we overexpressed Avr1d (without signal peptide) fused with an N-terminal enhanced green fluorescence protein (eGFP) in soybean hairy roots and performed infection assays using mRFP-labeled *P. sojae*. *P. sojae* infection was evaluated by quantifying the number of produced oospores and *P. sojae* biomass at 2 d postinoculation. Both the produced oospores and biomass of *P. sojae* were much greater in the hairy roots overexpressing eGFP-Avr1d than in the eGFP control (Fig. 1*A*). These results suggested that Avr1d could promote *P. sojae* infection.

To confirm secretion of Avr1d by *P. sojae*, Avr1d with native signal peptide fused with monomeric red fluorescence protein (mRFP) at the C terminus was overexpressed in the wild-type *P. sojae* strain P6497. The mRFP-labeled *P. sojae* was used as a control (10). Protein expression was confirmed by Western blot with anti-mRFP (*SI Appendix*, Fig. S1). Confocal microscopy visualization of infected hypocotyl epidermal cells showed that the red fluorescence of Avr1d-mRFP concentrated specifically at the haustoria, while the control mRFP localized in the cytosol, without significant concentration in the haustoria (Fig. 1*B*). This result suggested that the haustoria were primary sites of Avr1d secretion during infection.

Avr1d Physically Interacts with GmPUB13 In Vitro and In Vivo. To uncover the molecular mechanism underlying the function of Avr1d in promoting *P. sojae* infection, we performed yeast two-hybrid screening to identify potential soybean targets of Avr1d. Through screening, we identified two highly homologous genes, Glyma12g06860 and Glyma11g14910 that encode U-box ARM-repeats-type E3 ligases. Phylogenetic analysis indicated that these two genes were homologous to AtPUB13 of *A. thaliana* (*SI Appendix*, Fig. S2*A*). Glyma12g06860 and Glyma11g14910 shared 97.0% amino acid sequence identity (*SI Appendix*, Figs. S2*B* and S3*A*) and we named them GmPUB13 and GmPUB13L, respectively. Further, yeast two-hybrid assays supported that Avr1d interacted with both GmPUB13 and GmPUB13L (Fig. 1*C*). In support of the interaction between Avr1d and GmPUB13, we coexpressed Avr1d and GmPUB13 in *Nicotiana benthamiana* and found eGFP-Avr1d and GmPUB13-HA-mRFP colocalized to the cytoplasm under the confocal fluorescence microscopy (Fig. 1*D*). Furthermore, GmPUB13-HA-mRFP coimmunoprecipitated from *N. benthamiana* cell extracts with eGFP-Avr1d, but not with eGFP (Fig. 1*E*). To determine whether Avr1d physically interacted with GmPUB13 in vitro, we performed pull-down assays and found His-GmPUB13 could be pulled down by GST-Avr1d, but not by GST (Fig. 1*F*). The physical interaction between Avr1d and GmPUB13 was further confirmed by gel filtration chromatography (*SI Appendix*, Fig. S3*B*). Together, these data demonstrated that Avr1d physically interacted with GmPUB13 both in vivo and in vitro.

Crystal Structure of the Complex of Avr1d with the GmPUB13 U-Box Domain. Avr1d belongs to the class of RxLR effectors that carry a signal peptide followed by the RxLR motif and an effector domain (*SI Appendix*, Fig. S4*A*) (9). To characterize the molecular mechanism by which Avr1d contributes to the virulence of *P. sojae*, we ascertained the structure of the effector domain of Avr1d complexed with the U-box domain of GmPUB13 (Fig. 2*A* and *SI Appendix*, Fig. S4*A*). The structure of the complex was determined at 2.5-Å resolution using single wavelength anomalous diffraction. The model was refined to final R_{work} and R_{free} values of 23.5% and 24.9%, respectively (*SI Appendix*, Table S1). The asymmetrical unit of the crystals contained one Avr1d-GmPUB13 U-box complex (PDB: 7C96).

Avr1d displayed the structural characteristic of a WY motif, adopting a three alpha helix bundle, in which the highly conserved Trp96 and Try118 formed a hydrophobic core. It shared structural similarity with Avr3a11 (3ZR8) (11), another WY motif-containing RxLR effector protein, yielding a root-mean-square deviation (rmsd) of 1.95 Å, despite low sequence similarity (*SI Appendix*, Fig. S4*B*).

The U-box domain of GmPUB13 consisted of a central α-helix (α1), a C-terminal helix (α2), a small antiparallel β-sheet (β1 and β2) and two prominent loops (loop1 and loop2) (Fig. 2*A*), resembling the structure of the U-box of the eukaryotic ubiquitin ligase, the C-terminus of Hsp70 interacting protein (CHIP) (PDB: 2OXQ) (12); it could be superimposed well with the CHIP U-box with a rmsd of 1.66 Å over 72 matching Cα atoms (Fig. 2*B*). The hydrophobic groove formed by loop1, loop2, and central α-helix α1 of GmPUB13 U-box contributed to the interaction with Avr1d. Five residues of GmPUB13, P264, I265, L267 (from loop1), W290 (from helix α1), and P299 (from loop2) formed hydrophobic interactions with five residues of Avr1d, I87, F90, F93 (from helix α2), A117, and I120 (from helix α3). In addition to the hydrophobic interactions, hydrogen bonds and a salt bridge formed between GmPUB13 D259 and Avr1d R123 also stabilized the complex (Fig. 3*A*). Intriguingly, the residues in CHIP corresponding to the Avr1d-binding residues of GmPUB13 in CHIP are F218, I216, H241, and P250, and these four residues are necessary for the interaction of CHIP with the E2 subunit, UbcH5a (*SI Appendix*, Fig. S4*C*) (12). Therefore, by similarity to the UbcH5a-CHIP complex, the Avr1d-binding site of GmPUB13 was predicted also to be its E2 binding site, and suggesting that Avr1d may compete with E2 for GmPUB13 binding. Using yeast two-hybrid screening over 35 soybean E2s (GmE2s) from 14 different groups, we found seven GmE2s could interact with GmPUB13 (*SI Appendix*, Fig. S5*A*). As expected, the GmPUB13-Avr1d-binding affinity was stronger than those of GmPUB13-GmE2s in the yeast two-hybrid assay (*SI Appendix*, Fig. S5*B*). Two of the seven GmE2s and Avr1d were further assayed for the binding affinity with GmPUB13 using the isothermal titration calorimetry (ITC) assay. As shown in Fig. 2*C* and *SI Appendix*, Fig. S5*C*, the binding affinity of GmPUB13-Avr1d (K_d 89 nM) was much stronger than those of GmPUB13-GmE2s (K_d 39.1 μM and 46.6 μM). Altogether, these results suggested that Avr1d tightly occupied the E2-binding site of GmPUB13 to compete with E2 for GmPUB13 binding.

The Phenylalanine 90 of Avr1d Is Required for Interaction with GmPUB13 and Virulence Function. The crystal structure revealed that hydrophobic interactions played major roles in Avr1d-GmPUB13 complex formation, in which the phenyl ring of Avr1d F90 inserted into the hydrophobic groove formed by P264, I265, W290, and P299 of GmPUB13 (Fig. 3*A*). Substitution of these residues in GmPUB13, P264, I265, W290, and P299, with alanine, compromised Avr1d binding (*SI Appendix*, Fig. S6*A*). On the other side, the mutation F90A in Avr1d likewise disrupted GmPUB13 binding as measured by ITC, gel filtration, and yeast two-hybrid assays, indicating that F90 was essential for the interaction with GmPUB13 (Fig. 3*B* and *SI Appendix*, Fig. S6 *A* and *B*). To evaluate the effect of this mutation on the potential virulence contribution of Avr1d, we overexpressed $Avr1d^{F90A}$ and wild-type Avr1d in soybean hairy roots, then inoculated the roots with mRFP-labeled *P. sojae*. We observed that *P. sojae* oospore production in hairy roots expressing $Avr1d^{F90A}$ was

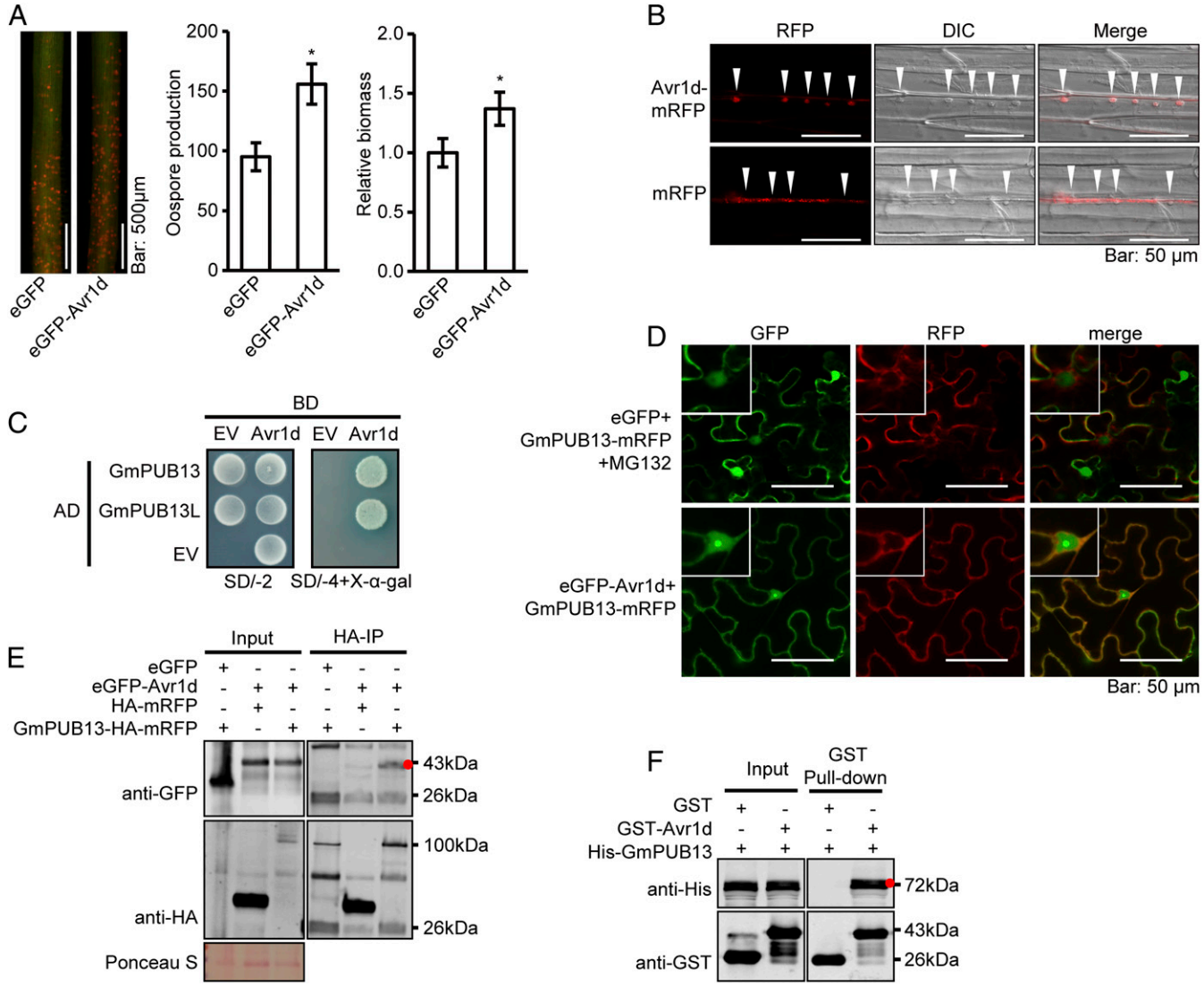

Fig. 1. Avr1d promotes *P. sojae* infection and targets to GmPUB13. (*A*) Overexpression of Avr1d in soybean hairy roots promotes *P. sojae* infection. The fluorescent hairy roots expressing eGFP or eGFP-Avr1d were inoculated with mRFP-labeled *P. sojae* hyphae plugs on the tips (*Left*). (Scale bar, 500 μm.) The oospore production was observed under fluorescence microscopy (*Middle*). Relative biomass of *P. sojae* was determined by qPCR at 48 h postinoculation (hpi) (*Right*). Asterisks indicated *t* test $P < 0.05$. These experiments were repeated three times with similar results. (*B*) Avr1d is secreted through haustoria. The etiolated soybean seedlings were inoculated with *P. sojae* zoospore expressing Avr1d-mRFP or mRFP. Triangles indicate *P. sojae* haustoria. (Scale bar, 50 μm.) (*C*) The interaction of Avr1d with GmPUB13 and GmPUB13L in yeast. Avr1d interacted with GmPUB13 and GmPUB13L, as indicated by yeast two-hybrid assays. EV, empty vector; SD/−2 medium: SD/−Leu/−Trp medium; SD/−4 + X-α-gal: SD/−Ade/−His/−Leu/−Trp + X-α-gal medium. (*D*) eGFP-Avr1d and GmPUB13-HA-mRFP colocalized at cytoplasm in *N. benthamiana* cells. eGFP and GmPUB13-HA-mRFP were coexpressed in *N. benthamiana* leaves (infiltrated with 50 μM MG132 12 h before observation) by agroinfiltration. eGFP-Avr1d and GmPUB13-HA-mRFP were coexpressed in *N. benthamiana* leaves by agroinfiltration. The leaves were observed under confocal microscopy 2 d postinfiltration. The smaller pictures on the *Upper Left* are a bigger view of the nucleus region in the main picture. (Scale bar, 50 μm.) (*E*) Confirmation of the interaction between Avr1d and GmPUB13 by Co-IP. Pairs of eGFP and GmPUB13-HA-mRFP, eGFP-Avr1d and HA-mRFP, and eGFP-Avr1d and GmPUB13-HA-mRFP were coexpressed in *N. benthamiana* leaves, respectively. Total protein extractions of the leaves were incubated with agarose beads conjugated anti-HA mouse monoclonal antibody followed by washing with PBS buffer five times. Proteins in each sample were detected by Western blot with anti-GFP and anti-HA antibodies. Red dot indicated the protein size of eGFP-Avr1d. Ponceau S: Ponceau staining indicates the rubisco protein. Molecular mass markers are shown (in kilodaltons). (*F*) Confirmation of the interaction between Avr1d and GmPUB13 by GST pull-down. Protein extracts of GST-Avr1d and His-GmPUB13 or GST-tag and His-GmPUB13 were mixed and incubated with glutathione Sepharose 4B beads, respectively, and followed by washing with PBS buffer five times. Proteins in the input samples and pull-down samples were detected by Western blot with anti-His and anti-GST antibodies. Red dot indicated the protein size of His-GmPUB13. Molecular mass markers are shown (in kilodaltons).

not significantly different from in hairy roots expressing eGFP (Fig. 3*C*). Avr1d^{F90A} protein expression in the transformed hairy roots was confirmed by Western blotting with anti-GFP antibodies (*SI Appendix*, Fig. S7). Thus, Avr1d^{F90A} failed to promote *P. sojae* infection. Together, these results demonstrated that F90 of Avr1d was required for the interaction with GmPUB13 and for its potential virulence contribution.

Avr1d Inactivates the Ubiquitin Ligase Activity of GmPUB13 In Vitro and In Vivo. According to our structure and biochemical assays, Avr1d could compete with E2 for GmPUB13 binding. To determine whether Avr1d affects the ubiquitin ligase activity of GmPUB13, we performed a ubiquitination assay using GmPUB13 as E3 in vitro. The smeared bands detected by ubiquitin antibodies following Western blotting indicated that polyubiquitin chains of different molecular weights had been formed (Fig. 4*A*). In contrast,

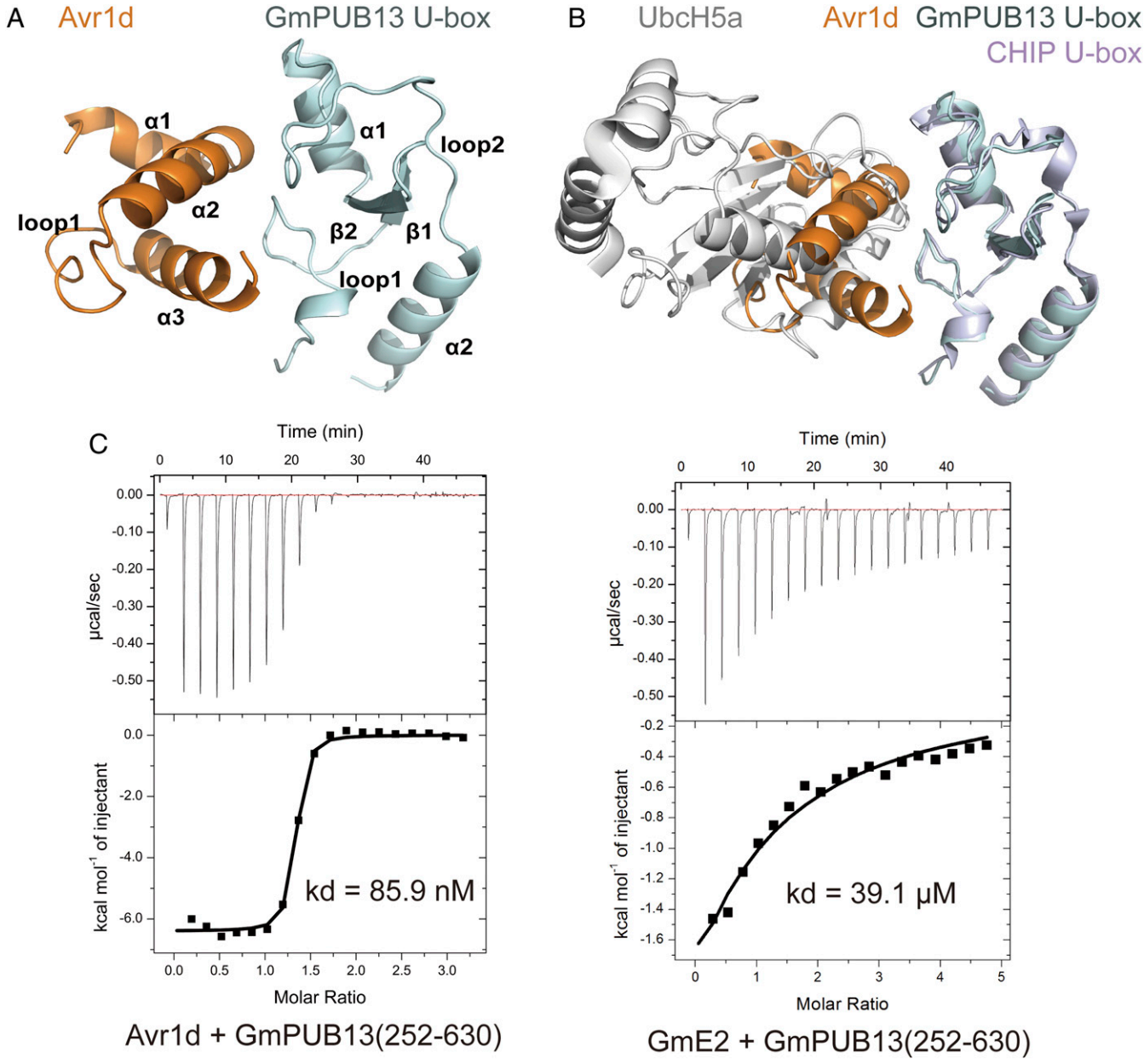

Fig. 2. Avr1d interacts with GmPUB13 by occupying the E2-binding site of GmPUB13. (*A*) Overall structure of Avr1d-GmPUB13 U-box. Avr1d (orange) and GmPUB13 U-box (cyan) are shown in cartoon form. (*B*) Superposition of crystal structures of Avr1d-GmPUB13 U-box and UbcH5a-CHIP U-box (PDB: 2OXQ). Avr1d (orange), GmPUB13 U-box (cyan), UbcH5a (gray), and CHIP U-box (blue white) are shown in cartoon form. (*C*) Binding affinity of Avr1d or GmE2 with GmPUB13. ITC-binding curve between Avr1d and GmPUB13(252 to 630) (*Left*). ITC-binding curve between GmE2 and GmPUB13(252 to 630) (*Right*). The ITC experiments were repeated twice independently with similar results. GmE2: Glyma06g13020.

no smeared bands were detected in the reaction containing E1, E2, GST, or in the reactions containing GmPUB13 but lacking E1 or E2 (Fig. 4*A*), showing GmPUB13 was an active ubiquitin ligase. It has been reported that cysteine 262 and tryptophan 289 of AtPUB13 in the U-box domain are required for its ligase activity (5). GmPUB13 with mutations on these sites, such as GmPUB13^{C263A} or GmPUB13^{W290A} lost ubiquitin ligase activity since no smeared bands of polyubiquitin were detected in these reactions (Fig. 4*A*), supporting the importance of the U-box domain for enzyme activity. To test whether Avr1d could modulate the enzyme activity of GmPUB13, Avr1d was added into the reaction mixture. The smeared bands were much weaker compared with the control (Fig. 4*B*). Thus, Avr1d indeed inhibited ubiquitin ligase activity of GmPUB13. In line with this, Avr1d decreased the ubiquitin ligase activity of GmPUB13 in a dose-dependent manner since the smeared polyubiquitin bands became progressively weaker as the concentration of Avr1d was increased (Fig. 4*B* and *SI Appendix*, Fig. S8*A*). However, even high amounts of Avr1d^{F90A} protein could not block the ubiquitin ligase activity of GmPUB13 since Avr1d^{F90A} failed to bind GmPUB13 (Fig. 4*C* and *SI Appendix*, Fig. S8*B*). To further evaluate the effect of Avr1d on the ligase activity of GmPUB13, we performed a ubiquitination assay in *N. benthamiana*. In line with our in vitro assay, smeared bands of polyubiquitin in leaves coexpressing Avr1d and GmPUB13 were weaker than that in leaves expressing GmPUB13 and eGFP or Avr1d^{F90A} with similar amount of GmPUB13 protein loaded, respectively (Fig. 4*D* and *SI Appendix*, Fig. S8*D*). Altogether, Avr1d inhibited the ubiquitination activity of GmPUB13 in vitro and in vivo. GmPUB13 and

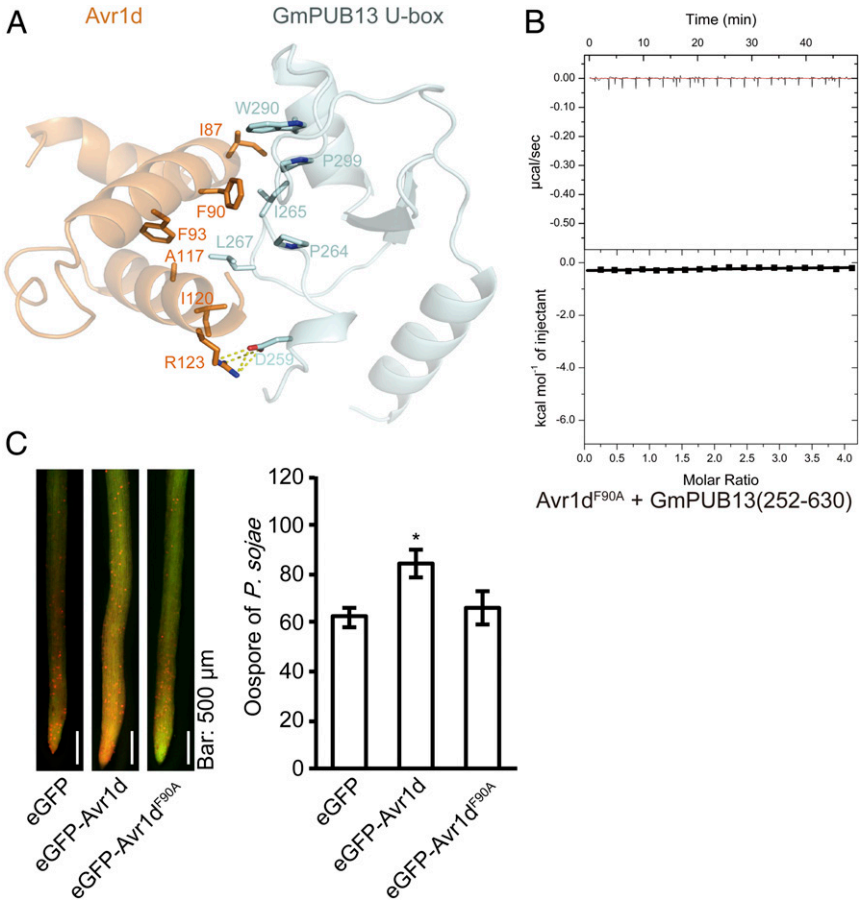

Fig. 3. The 90th F of Avr1d is the key residue for the interaction with GmPUB13 and its virulence function. (*A*) Interaction residues between Avr1d and GmPUB13. The I87, F90, F93, A117, and I120 of Avr1d (orange) contribute to the hydrophobic interaction surface with P264, I265, L267, W290, and P299 of GmPUB13 U-box (cyan). R123 of Avr1d (orange) forms hydrogen bonds and salt bridge with D259 of GmPUB13 U-box (cyan). (*B*) ITC-binding curve between Avr1d^{F90A} and GmPUB13(252 to 630). The ITC experiments were repeated twice independently with similar results. (*C*) Overexpression of Avr1d^{F90A} in soybean hairy roots fails to promote *P. sojae* infection. The fluorescence hairy roots expressing eGFP, eGFP-Avr1d, and eGFP-Avr1d^{F90A} were inoculated with mRFP-labeled *P. sojae* hyphae on the tips (*Left*). (Scale bar, 500 µm.) The oospore production was observed under fluorescence microscopy at 2 d postinoculation (*Right*). Asterisks indicate *t* test $P < 0.05$. These experiments were repeated three times with similar results.

GmPUB13L shared 97% sequence identity. Especially within the U-box domain, the region that interacts with Avr1d, the sequences are exactly the same (*SI Appendix*, Fig. S3*A*). In addition, we tried to test the interaction between Avr1d with GmPUB13L using gel filtration and in vitro ubiquitination assays. In these assays, Avr1d also interacted with GmPUB13L and inhibited its ubiquitin ligase activity (*SI Appendix*, Figs. S3*C* and S8*C*). Together, these data demonstrate that GmPUB13 and GmPUB13L probably function redundantly in soybean.

GmPUB13 Self-Ubiquitination Regulates Its Abundance. To explore whether GmPUB13 could regulate its protein abundance by self-ubiquitination, we expressed the inactive mutants GmPUB13^{C263A} and GmPUB13^{W290A} in *N. benthamiana* leaves. The protein abundance and fluorescence of GmPUB13^{C263A}-HA-mRFP, GmPUB13^{W290A}-HA-mRFP, and control HA-RFP were much stronger than GmPUB13-HA-mRFP (Fig. 4*E* and *SI Appendix*, Fig. S9 *A* and *B*). The protein abundance of GmPUB13-HA-mRFP was significantly increased when the infiltrated leaves were treated with 50 µM MG132, a 26S proteasome complex inhibitor (Fig. 4*F*). Together, these data suggest that GmPUB13 may regulate its protein abundance by self-ubiquitination and 26S proteasome-mediated degradation.

GmPUB13 Promotes Plant Susceptibility. To determine the role of GmPUB13 in soybean resistance, we silenced GmPUB13 and GmPUB13L in soybean hairy roots. The qRT-PCR assay revealed that GmPUB13/GmPUB13L gene expression level decreased around 60% in the silenced hairy roots with little effect on a homologous gene Glyma10g35220 when compared to the empty vector control (*SI Appendix*, Fig. S10 *A* and *B*). The GmPUB13/GmPUB13L silenced hairy roots showed less oospore production and *P. sojae* biomass compared to the control hairy roots when inoculated with eGFP-labeled *P. sojae* (Fig. 5*A*). In addition, the relative expression levels of several resistance-related marker genes, such as *GmPR1a*, *GmPR2*, and *GmPR3*, were slightly increased in GmPUB13/GmPUB13L silenced hairy roots (*SI Appendix*, Fig. S10*C*), suggesting that GmPUB13 and GmPUB13L are susceptibility factors for *P. sojae* (13). To further verify the conclusion, HA-GmPUB13 and derived mutants were overexpressed in soybean hairy roots. The protein abundance of GmPUB13 mutants was greater than wild-type GmPUB13 as detected by Western blot (Fig. 5*B*). The hairy roots were inoculated with mRFP-labeled *P. sojae* and Avr1d knockout *P. sojae* mutants (*SI Appendix*, Fig. S12 *A–D*). The results showed that the oospore production was slightly increased in the hairy roots expressing GmPUB13 than EV control when inoculated with mRFP-labeled *P. sojae*. There was also a slight, albeit not significant, increase of *P. sojae* biomass in the hairy

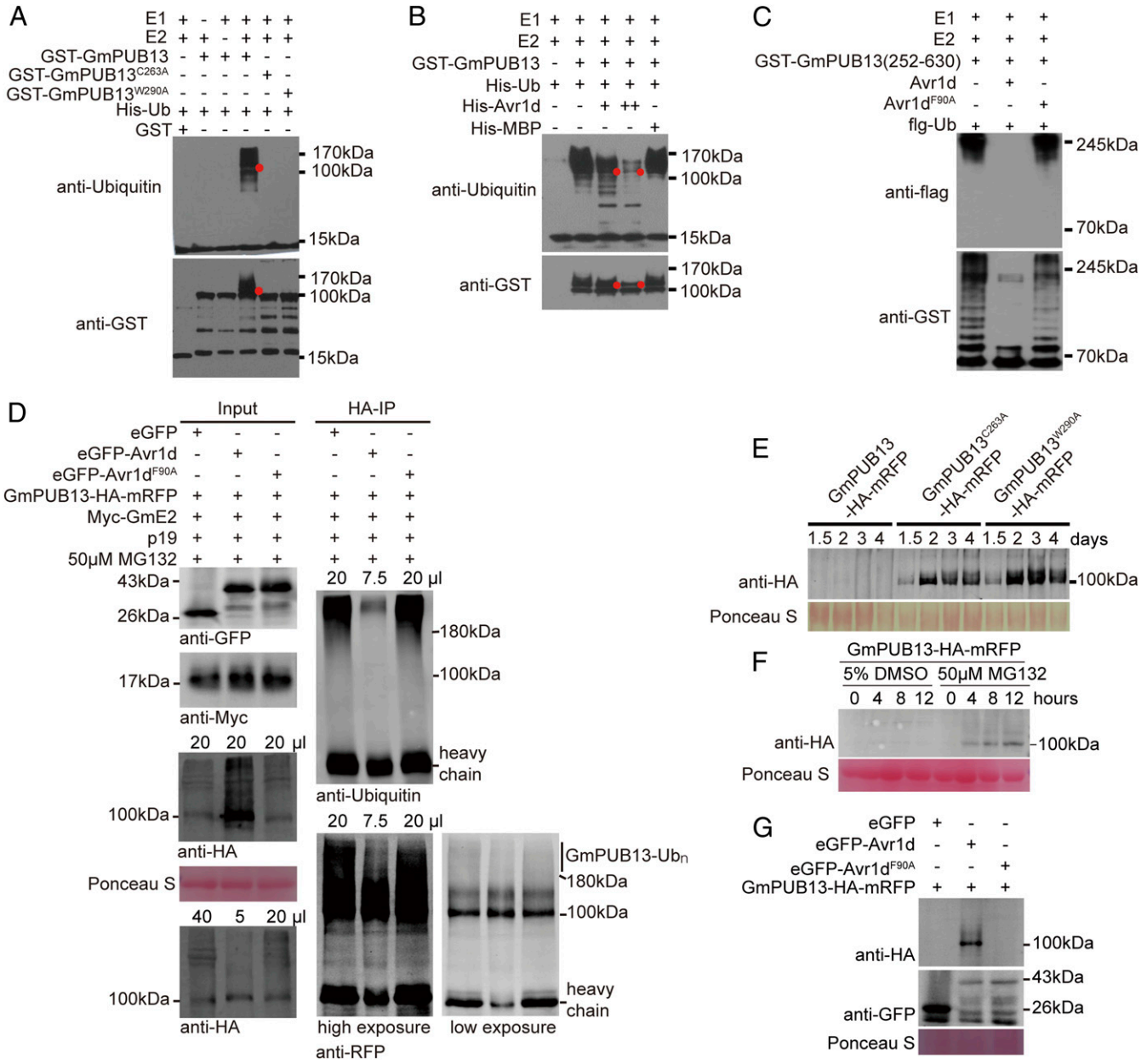

Fig. 4. Avr1d inhibits GmPUB13's ubiquitin ligase activity to promote its accumulation. (*A*) Ubiquitination assays of GmPUB13, GmPUB13^{C263A}, and GmPUB13^{W290A} in vitro. GmPUB13 and mutants were fused with GST-tag and incubated with or without wheat E1, AtUBC8 as E2 in the buffer with ubiquitin. Reaction mixtures were detected by Western blot with anti-ubiquitin and anti-GST. Red dots indicate the protein size of GST-GmPUB13. Molecular mass markers are shown (in kilodaltons). (*B*) Avr1d inhibits the ubiquitin ligase activity of GmPUB13. His-Avr1d and His-MBP proteins were added into the reaction mixtures with E1, E2, and GST-GmPUB13 as E3. Double plus (++) indicated double amount of His-Avr1d protein. Reaction mixtures were detected by Western blot with anti-ubiquitin and anti-GST. Red dots indicate the protein size of GST-GmPUB13. Molecular mass markers are shown (in kilodaltons). (*C*) Avr1d^{F90A} fails to inhibit the ubiquitin ligase activity of GmPUB13. Avr1d or Avr1d^{F90A} protein were respectively added into the reaction mixture with E1, the soybean predicted ubiquitin conjugating enzyme-related protein Glyma06g13020 as E2, flag-ubiquitin, and GST-GmPUB13(252 to 630) as E3. Reaction mixtures were detected by Western blot with anti-GST and anti-flag. Molecular mass markers are shown (in kilodaltons). (*D*) Avr1d inhibited the ubiquitination activity of GmPUB13 in *N. benthamiana*. eGFP, eGFP-Avr1d, and eGFP-Avr1d^{F90A} were coexpressed with GmPUB13-HA-mRFP, Myc-GmE2 (Glyma06g13020), and p19 in *N. benthamiana* leaves, respectively. Leaves were injected with 50 μM MG132 12 h before harvest. The input samples were detected by anti-HA, anti-Myc, and anti-GFP antibody and the output samples were detected by anti-RFP and anti-ubiquitin antibody. The smear bands indicate polyubiquitin chains. Ponceau S: Ponceau staining indicates the rubisco protein. Molecular mass markers are shown (in kilodaltons). (*E*) Protein accumulation of GmPUB13 and its mutants. GmPUB13-HA-mRFP, GmPUB13^{C263A}-HA-mRFP, and GmPUB13^{W290A}-HA-mRFP were expressed in *N. benthamiana* leaves by agroinfiltration, respectively. The total protein was extracted at 1.5, 2, 3, and 4 d postinfiltration followed by Western blot detection with anti-HA antibody. Ponceau S: Ponceau staining indicates the rubisco protein. Molecular mass markers are shown (in kilodaltons). (*F*) MG132 treatment increases GmPUB13-HA-mRFP protein abundance. The leaves expressing GmPUB13-HA-mRFP were infiltrated with 50 μM MG132 0, 4, 8, and 12 h before harvest and 0.5% DMSO as control. The total protein was detected by Western blot with anti-HA antibody. Ponceau S: Ponceau staining indicates the rubisco protein. Molecular mass markers are shown (in kilodaltons). (*G*) Avr1d, but not Avr1d^{F90A}, can stabilize GmPUB13. GmPUB13-HA-mRFP was coexpressed with eGFP, eGFP-Avr1d, or eGFP-Avr1d^{F90A} in soybean hairy roots. The total proteins of the hairy roots were detected by Western blot with anti-HA and anti-GFP. Ponceau S: Ponceau staining. Molecular mass markers are shown (in kilodaltons).

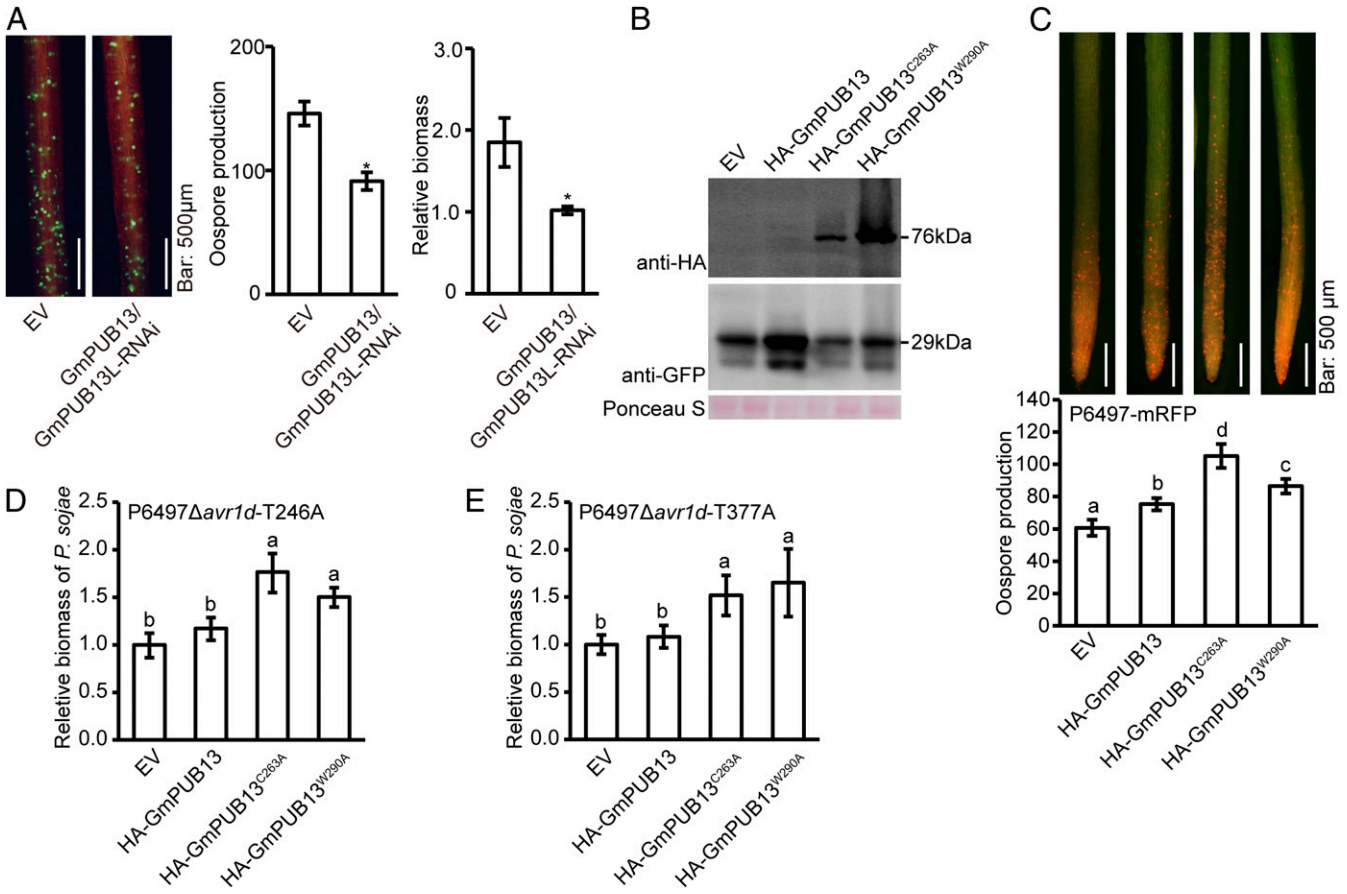

Fig. 5. Expression of inactivated GmPUB13 promotes *P. sojae* infection. (*A*) Silencing of GmPUB13 and GmPUB13L in soybean hairy roots by RNAi decreases *P. sojae* infection. GmPUB13 and GmPUB13L were silenced in soybean hairy roots by RNAi. The tips of red fluorescence hairy roots were inoculated with eGFP-labeled *P. sojae* hyphae plugs (*Left*). The oospore production was observed under fluorescence microscopy at 2 d postinoculation (*Middle*). The relative *P. sojae* biomass was estimated by DNA-based quantitative PCR (qPCR) (*Right*). Asterisks indicate *t* test $P < 0.05$. These experiments were repeated three times with similar results. (Scale bar, 500 μm.) (*B*) HA-GmPUB13 and derived mutants were coexpressed with eGFP in soybean hairy roots. The total protein of the hairy roots was detected by anti-GFP and anti-HA. Ponceau S: Ponceau staining. Molecular mass markers are shown (in kilodaltons). (*C*) Overexpression of inactivated GmPUB13 mutants in soybean hairy roots promotes *P. sojae* infection. The hairy roots overexpressed HA-GmPUB13 or GmPUB13 mutants were inoculated with mRFP-labeled *P. sojae*. The oospore production was observed under fluorescence microscopy. a, b, c, and d indicate *t* test $P < 0.05$. These experiments were repeated three times with similar results. (Scale bar, 500 μm.) (*D* and *E*) Overexpression of inactivated GmPUB13 mutants in soybean hairy roots promotes the infection of *Avr1d* knockout mutants. The hairy roots overexpressed HA-GmPUB13 or GmPUB13 mutants were inoculated with Avr1d knockout mutants T246A and T377A. The genome DNA of hairy roots was extracted and the relative *P. sojae* biomass was estimated by DNA-based quantitative PCR (qPCR). a and b indicate *t* test $P < 0.05$. These experiments were repeated three times with similar results.

roots expressing HA-GmPUB13 than EV control, when inoculated with Avr1d knockout mutants (Fig. 5 *C*–*E*). In addition, we found that the oospore production and *P. sojae* biomass was significantly increased in the hairy roots expressing GmPUB13^{C263A} or GmPUB13^{W290A} than expressing GmPUB13 or EV control when infected with mRFP-labeled *P. sojae* or Avr1d knockout mutants (Fig. 5 *C*–*E*). We also overexpressed GmPUB13-HA-mRFP and mutants in *N. benthamiana* leaves and then performed infection assays using *Phytophthora capsici*. Compared with the HA-mRFP control, *N. benthamiana* leaves expressing GmPUB13 showed no difference in lesion area (*SI Appendix*, Fig. S11*A*). However, the leaves expressing GmPUB13^{C263A} or GmPUB13^{W290A} showed much bigger lesions than those expressing GmPUB13 (*SI Appendix*, Fig. S11 *B* and *C*) or HA-mRFP control (*SI Appendix*, Fig. S11 *D* and *E*). These results suggested that the stable inactivated mutants of GmPUB13 could promote *P. sojae* and *P. capsici* infection when overexpressed in soybean hairy roots or *N. benthamiana* and that the inactive mutants did not need Avr1d to promote infection.

Avr1d Can Stabilize GmPUB13 In Planta. Since GmPUB13 could undergo self-ubiquitination to regulate its protein abundance and Avr1d inhibited the ubiquitination activity of GmPUB13, we tested whether Avr1d could stabilize GmPUB13 in planta. When we coexpressed Avr1d and GmPUB13 in soybean hairy roots, we observed that the red fluorescence of GmPUB13-HA-mRFP was stronger when coexpressed with Avr1d than with eGFP or Avr1d^{F90A} (*SI Appendix*, Fig. S13*A*). This also held true when GmPUB13-HA-mRFP was expressed with Avr1d, eGFP, or Avr1d^{F90A} in *N. benthamiana* (*SI Appendix*, Fig. S13*B*). We also detected stronger bands of GmPUB13-HA-mRFP in the total proteins of hairy roots or *N. benthamiana* leaves coexpressing GmPUB13-HA-mRFP with eGFP-Avr1d than with eGFP by anti-HA (Fig. 4*G* and *SI Appendix*, Fig. S13*C*). Unlike Avr1d, coexpressing Avr1d^{F90A} failed to stabilize GmPUB13 in soybean hairy roots and *N. benthamiana* leaves (Fig. 4*G* and *SI Appendix*, Fig. S13*C*). This is consistent with the previous results in Fig. 4 *B*–*D* suggesting that Avr1d could stabilize GmPUB13.

Discussion

Plant pathogens secrete large arsenals of effectors to modulate host cell processes and enable a successful infection. Studies on the host targets of such effectors provide molecular clues for

understanding the outcome of plant–pathogen interactions. Thus far, multiple host targets have been identified for effectors secreted by oomycete pathogens. However, structural evidence needed to unravel the mechanisms underlying interactions of effectors and host targets is still missing. In this study, we determined that *P. sojae* avirulence effector Avr1d physically binds to the soybean U-box-type E3 ligase GmPUB13 and we dissected the structural basis of this interaction.

A typical feature of most E3 ligases is the ability to catalyze their own ubiquitination. The biological role of self-ubiquitination was proposed to be to target the ligase for degradation, which could function as a means of negative feedback of E3 ligases (14, 15). In fact, many E3 ligases, even those that catalyze their own ubiquitination, are targeted by an exogenous ligase, which makes the regulation of E3 ligases rather complicated. In addition, self-ubiquitination of E3 ligases could be involved in nonproteolytic functions (16) and could enhance substrate ubiquitin ligase activity (17). In this study, we found that GmPUB13 was a substrate of its own E3 ubiquitin ligase activity and this self-ubiquitination induced degradation of GmPUB13 by the proteasome.

Ubiquitination contributes crucially to the intricate and precise molecular mechanisms that govern plant immune responses and therefore the ubiquitination system is a hub targeted by multiple pathogen virulence effectors. For example, several effectors possess E3 ubiquitin ligase activity, such as AvrPtoB from *Pseudomonas syringae* (18, 19) and XopK from *Xanthomonas oryzae pv. oryzae* (20) that degrade host targets to attenuate plant immunity.

In addition, effectors may hijack the host ubiquitination complex to reprogram the stability of host targets. AvrPiz-t from *Magnaporthe oryzae* interacts with the RING-type E3 ubiquitin ligase APIP6, a positive regulator of rice immunity, to promote the degradation of APIP6 (21). The *Phytophthora infestans* RxLR effector Pi02860 interacts with a potato susceptibility factor StNRL1, a putative substrate adaptor of a CULLIN3-associated ubiquitin E3 ligase complex, to degrade a guanine nucleotide exchange factor called SWAP70, which is essential for potato immunity (22, 23). In addition, *P. infestans* effector AVR3a interacted with a U-box-type ubiquitin E3 ligase CMPG1 and manipulated plant immunity by stabilizing potato CMPG1 (24). Nevertheless, how AVR3a mediates the stability of CMPG1 is thus far unclear.

In this study, we found that the *P. sojae* avirulence effector Avr1d physically binds to the soybean U-box-type E3 ligase GmPUB13 and could stabilize GmPUB13 by suppressing its ubiquitin ligase activity. We deciphered the molecular mechanism underlying inhibition of GmPUB13 by Avr1d by determining the molecular structure of the Avr1d-GmPUB13 complex, combined with biochemical assays. Based on the crystal structure, we successfully identified the interface required for interaction between GmPUB13 and Avr1d and showed that the residues at the interface were required for Avr1d to bind to GmPUB13 and inhibit its ligase activity. Since GmPUB13 functions as a susceptibility factor, stabilization of GmPUB13 by Avr1d-mediated inhibition of its ligase activity is the key to the contribution of Avr1d to *P. sojae* virulence.

Materials and Methods

***Phytophthora*, Bacteria, and Plant Growth Condition.** *P. sojae* and *P. capsici* were grown in 10% (V/V) V8 medium with 1.5% agar or without agar in the dark at 25 °C. *Escherichia coli* JM109 for vector construction were grown on Luria–Bertani (LB) medium with agar or shaking 220 rpm in the dark without agar, 37 °C. *Agrobacterium tumefaciens* and *Agrobacterium rhizogenes* were grown on LB medium with 1.5% agar or with shaking 220 rpm in the dark without agar containing 50 μg/L rifampicin or streptomycin, respectively, at 30 °C. *N. benthamiana* were grown on vermiculite from seeds in a climate chamber under long-day conditions (14 h light and 10 h dark) at 24 °C. *Glycine max* etiolated seedlings were grown on vermiculite medium from seeds in the dark, at 25 °C for 3 to 4 d in a climate chamber.

***P. sojae* Transformation, Zoospore Producing, and Infection Assay.** Avr1d-mRFP driven by the Ham34 promoter (pTORmRFP4) was transformed into *P. sojae* strain P6497 using a PEG (polyethylene glycol)-mediated protoplast transformation system (25). Transformants were selected on 10% (V/V) V8 medium containing 50 μg/L geneticin (G418) and further confirmed by red fluorescence selection under fluorescence microscopy and Western blot detection of Avr1d-mRFP protein by anti-mRFP antibody. Avr1d was knocked out using the CRISPR/Cas9 system mediated gene editing following the protocols described by Fang et al. (26). The tranformants were screened by PCR using the genome DNA of transformants with primers listed in *SI Appendix*, Table S2. Mutants were confirmed by sequencing. *P. sojae* zoospores were produced by washing the 3- to 5-d-old *P. sojae* hyphae grown in 10% V8 liquid medium with sterilized tap water three times and then incubated in the dark (25 °C) to stimulate sporulation and zoospore releasing. The droplets containing about 100 zoospores were then inoculated to the hypocotyl of soybean etiolated seedlings. The inoculated samples were kept in wet and dark conditions at 25 °C. For a 5- to 10-h infection, the epidermal cells of soybean hypocotyl were observed under confocal microscopy.

Hairy Roots Transformation and Infection Assay. Soybean hairy root transformation was performed by using *A. rhizogenes* K599-mediated T-DNA transformation (27). Cotyledons of 6-d-old soybeans grown under long-day conditions (14 h light and 10 h dark) at 25 °C on vermiculite were used as explant for transformation. The lower epidermis of the cotyledons was wounded by cutting a 3- to 5-mm diameter wound. The wounding sites were inoculated with K599 strains carrying cognate plasmids for overexpression or silencing. After incubation for 3 to 4 wk on Murashige and Skoog (MS) medium at 25 °C, hairy roots were grown from the callus of the wounded sites. The transformed hairy roots were chosen under fluorescent microscopy.

To express Avr1d and the related mutants in the soybean hairy root, each was fused with N terminus eGFP and cloned into the T-DNA region of pBinGFP2 plasmid with the CaMV 35S promoter. To coexpress eGFP, eGFP-Avr1d, or eGFP-Avr1d^{F90A} with GmPUB13-HA-mRFP in soybean hairy roots, eGFP and GmPUB13-HA-mRFP, eGFP-Avr1d and GmPUB13-HA-mRFP, and eGFP-Avr1d^{F90A} and GmPUB13-HA-mRFP were cloned into two open reading frames separately in the T-DNA region of pFGC5941 plasmid driven by mannopine synthase promoter or cauliflower mosaic virus promoter (CaMV 35S), respectively. The green fluorescence hairy roots selected under fluorescence microscopy were regarded as transformed hairy roots. The protein expression of the fluorescence hairy roots was detected by Western blot with anti-GFP (CMC tag) or anti-HA.

For silencing of *GmPUB13* and *GmPUB13L* in soybean hairy roots, a 100-bp cDNA sequence that specifically matches to GmPUB13 and GmPUB13L (blasted by the VIGS tool in https://solgenomics.net/) was constructed with forward and reverse sequence linked by chalcone synthase intron from *Petunia hybrida* into pFGC5941mCherry plasmid with CaMV 35S promoter. The T-DNA region contains another open reading frame for mCherry expression driven by a mannopine synthase promoter. The red fluorescence hairy roots under fluorescence microscopy were regarded as silenced hairy roots. The total RNA was extracted using the Total RNA Kit (Cat. No. R6834, OMEGA). The silencing efficiency and the relative expression levels of resistance-related marker genes were detected by real-time quantitated PCR (qPCR) by relative to the gene expression of *GmCYP2* (8).

To test the susceptibility of transformed soybean hairy roots, more than 30 transformed hairy roots were collected and infected with eGFP or mRFP-labeled *P. sojae*. The hairy roots were incubated in humid and dark conditions for 2 d at 25 °C (28). The oospore production was assayed under fluorescence microscopy. The relative biomass of *P. sojae* grown in transformed hairy roots was detected by quantitative PCR and indicated by the ratio of *P. sojae* actin gene and soybean *GmCYP2* gene.

Yeast Two-Hybrid Assay. The PEG-mediated transformation protocol described in the Clontech Yeast Protocol Handbook was used to transform plasmids into yeast AH109 and Matchmaker GAL4 two-hybrid system to screen for targets or check the protein-to-protein interaction. To screen host targets of Avr1d, Avr1d without signal peptide was constructed into vector pGBKT7 as the bait. cDNA libraries derived from soybean hypocotyl and root RNA were constructed to pGADT7 plasmid fused with GAL4 activation domain (AD) by the Clontech company. A total of 6×10^6 clones were screened. The yeast clones were selected on SD/−His/−Leu/−Trp medium for medium stringency interaction or on SD/−Ade/−His/−Leu/−Trp/X-α-Gal medium for high stringency interaction. The AD plasmids of the selected clones were extracted by Solarbio Plasmid Extraction Mini Kit (Cat. No. D1100) and were subsequently transformed into *E. coli* JM109 before sending to sequence. The obtained sequences were used to search in the phytozome (https://phytozome.jgi.doe.gov/pz/portal.html) database for candidate target genes. To

confirm the interaction of Avr1d or E2 conjugating enzyme-related genes and full-length GmPUB13, Avr1d and E2 conjugating enzyme-related genes were constructed into pGBKT7 plasmid, while full-length GmPUB13 and GmPUB13L were constructed into pGADT7 plasmid from soybean cDNA. The plasmids were cotransformed into yeasts and then tested on SD/−Leu/−Trp medium and SD/−Ade/−His/−Leu/−Trp/X-α-Gal medium.

GST Pull Down and Co-IP Assay. For GST pull down, Avr1d was cloned into pGEX 4T-2 with a C terminus GST tag, while GmPUB13 was cloned into pET28a fused with a C-terminal His-tag. Both Avr1d and GmPUB13 were expressed in *E. coli* BL21, induced by 0.2 mM IPTG (isopropyl-β-D-thiogalactopyranoside). The bacteria lysate containing GST-Avr1d was incubated with 10 μL glutathione Sepharose 4B beads (Cat. No. 45-000-139, GE Healthcare) for 3 h and purified by washing with 1 × PBS (phosphate buffered saline, Cat. No. ST448, Beyotime Biotechnology) five times. Then the beads were incubated with bacteria lysate containing His-GmPUB13 for another 3 h and purified by washing with PBS five times. The proteins eluted from the beads were determined by Western blot with anti-GST and anti-His. For Co-IP, Avr1d without signal peptide was cloned into pBinGFP2 plasmid fused with eGFP at its C terminal and GmPUB13 was cloned into pFGC5941HAmRFP fused with 3× HA-mRFP at its C terminal. Avr1d and GmPUB13 were coexpressed in *N. benthamiana* leaves by *A. tumefaciens*-mediated transformation. The total protein of *N. benthamiana* leaves was extracted in IP buffer (50 mM Tris·HCl pH = 7.5, 150 mM NaCl, 10% glycerol, 0.1% Triton X-100, 1% protease inhibitor cocktail [Cat. No. P9599, Sigma-Aldrich], 1 mM PMSF [phenylmethylsulfonyl fluoride]) and then incubated for 4 h with 10 μL agarose beads conjugated anti-HA mouse monoclonal antibody (Cat. No. AT0079, CMC tag). After washing with 1× PBS buffer five times, the agarose beads with proteins were boiled in 1× SDS (sodium dodecyl sulfate)-PAGE (polyacrylamide gel electrophoresis) loading buffer for 10 min. Then the protein samples were determined by Western blot with anti-HA (Abmart) and anti-GFP (CMC tag).

Relative Quantification of *P. sojae* Biomass. The genome DNA of infected soybean hairy roots was extracted using the New Plant Genome Extraction Kit (Cat. No. DP305, Tiangen Biotech) and used for qPCR with ChamQ SYBR qPCR Master Mix (Cat. No. Q311, Vazyme). The *P. sojae* biomass was calculated by using the *P. sojae PsActin* gene relative to the soybean *GmCYP2* gene. Primer sequences are listed in *SI Appendix*, Table S2.

Transient Expression in *N. benthamiana*. Avr1d, GmPUB13, and related mutant sequences were amplified by Phanta Max Super-Fidelity DNA Polymerase (Cat. No. P505, Vazyme) from cDNA of *P. sojae* or *G. max*, respectively. The fragments were then cloned into vector pBinGFP2 or pFGC5941HAmRFP using ClonExpress II One Step Cloning Kit (Cat. No. C112, Vazyme). *A. tumefaciens* strains with different plasmids were infiltrated into *N. benthamiana* leaves. The leaves were harvested 1.5, 2, 3, and 4 d postinfiltration. Total proteins were extracted in IP buffer (50 mM Tris·HCl pH = 7.5, 150 mM NaCl, 10% glycerol, 0.1 to 1% Triton X-100, 1% protease inhibitor cocktail, 1 mM PMSF). The proteins of different samples were determined by Western blot with anti-HA or anti-HA (Abmart) and anti-GFP (CMC tag).

MG132 Treatment. MG132, a 26S proteasome inhibitor, was dissolved in dimethyl sulfoxide (DMSO) with a concentration of 10 mM. MG132 diluted in 10 mM $MgCl_2$ buffer with a final concentration of 50 μM was infiltrated into *N. benthamiana* leaves 0, 4, 8, 12 h before harvested. A total of 5% DMSO diluted in 10 mM $MgCl_2$ buffer was infiltrated as control.

Inoculation with *P. capsici* on *N. benthamiana* Leaves. *A. tumefaciens* strain pairs for expressing HA-mRFP and GmPUB13, HA-mRFP and GmPUB13 mutants, or GmPUB13 and mutants were infiltrated into the two sides of *N. benthamiana* leaves (>18 leaves), respectively. Then 36 h postinfiltration, infiltrated leaves were inoculated with mycelia plugs of fresh *P. capsici* (plug diameter was about 5 mm) and kept in the dark with high humidity for 2 d. The disease symptoms were visualized under ultraviolet (UV) light.

Ubiquitination Assay In Vitro. Ubiquitination assay in vitro was carried out following the protocol described by Zhao et al. (29). Wheat E1 protein, AtUBC8, and the predicted soybean E2 Glyma06g13020 were expressed in *E. coli* BL21 and purified by Ni NTA beads. GmPUB13 or GmPUB13(252-630) and other mutants fused with GST-tag were expressed in *E. coli* BL21 and purified by immunoprecipitation with glutathione Sepharose 4B beads (Cat. No. 45-000-139, GE Healthcare). Each reaction with 30 μL final volume contained 50 ng wheat E1 protein, 200 to 500 ng AtUBC8 or the predicted soybean E2 Glyma06g13020 protein as E2 conjugating enzyme, 5 μg ubiquitin together with reaction buffer (50 mM Tris·HCl pH 7.4, 10 mM $MgCl_2$, 5 mM dithiothreitol, 5 mM ATP, 10% glycerol) in the tubes containing beads binding with GmPUB13, mutants, or GST-tag proteins. The reactions were incubated in a thermomixer for 3 h at 30 °C with shaking and stopped by adding 1× SDS-PAGE loading buffer and incubated for another 5 min at 100 °C. Avr1d and Avr1d^{F90A} aliquoting (5 μL) for each reaction were analyzed by electrophoresis on 12% SDS-PAGE gels. The incubated mixtures were detected by Western blot using anti-ubiquitin (Abcam), anti-GST (Abmart), and anti-Flag (Abmart).

The Inhibition of Ubiquitin Ligase Activity in *N. benthamiana*. eGFP, eGFP-Avr1d, and eGFP-Avr1d^{F90A} were coexpressed with GmPUB13-HA-mRFP, as well as Myc-Glyma06g13020 (a ubiquitin-conjugated enzyme protein-related gene) and p19 in *N. benthamiana* leaves, respectively. *A. tumefaciens* strains with cognate plasmids was washed three times using 10 mM $MgCl_2$ buffer with 10 mM (4-morpholineethanesulfonic acid) (pH 5.7) and 100 μM acetosyringone. The final concentration of OD_{600} was 0.4 (for GmPUB13-HA-mRFP), 0.2 (for GFP-Avr1d, GFP-Avr1d^{F90A}), or 0.1 (for p19). *N. benthamiana* plants were grown in a climate chamber for 2 d after infiltration. Leaves were injected with 50 μM MG132 in 10 mM $MgCl_2$ buffer 12 h before harvest. The total protein was extracted in TBS (Tris buffered saline) 300 buffer (50 mM Tris·HCl pH = 7.5, 300 mM NaCl) with 0.1% Triton X-100, 1% protease inhibitor cocktail, and 50 μM MG132. The homogenized samples were centrifuged twice using 13,000 × *g* for 10 min and the protein supernatants of each sample were incubated with 10 μL agarose beads conjugated anti-HA mouse monoclonal antibody (Cat. No. AT0079, CMC tag) for 4 h. The beads were then washed with TBS 500 buffer (50 mM Tris·HCl pH = 7.5, 500 mM NaCl) four times and boiled in 100 °C for 5 min in SDS-PAGE loading buffer. The input samples were determined by Western blot with anti-HA (Abmart), anti-myc (Abmart), and anti-GFP (CMC tag) and the output samples were determined by Western blot with anti-RFP (Cat. No. 6G6, ChromoTek) and anti-ubiquitin (Cat. No. ab7254, Abcam).

Protein Expression and Purification. The GmPUB13 U-box and Avr1d were both cloned into the modified pET32a vector (Novagen) after adding a cleavage site for the tobacco etch virus (TEV) protease to the 5′ and 3′ ends of the Avr1d and GmPUB13 gene through PCR amplification. For His-GmPUB13 U-box and Avr1d protein coexpression, the constructs were transformed into *E. coli* BL21(DE3), and cells were grown at 37 °C to OD_{600} = 0.6 to 0.8 and induced with 0.1 mM IPTG for 8 to 10 h at 16 °C. The cells were harvested by centrifugation for 15 min at 4,000 × *g* at 4 °C. Cells were resuspended in Ni-lysis buffer (50 mM Tris [pH 8.0], 200 mM NaCl, 20 mM imidazole) and lysed with a homogenizer. The lysate was centrifuged for 1 h at 17,000 × *g* (4 °C), and the supernatant was passed over a Ni-affinity column (GE Healthcare). His-GmPUB13 U-box and Avr1d were recovered by gradient elution with Ni-elution buffer (50 mM Tris [pH 8.0], 200 mM NaCl, 200 mM imidazole). Fractions containing His-GmPUB13 U-box and Avr1d were verified by SDS-PAGE and pooled for tag cleavage to cleave the His tag overnight at 4 °C with 1:20 tobacco etch virus (TEV) protease. The tag-removed His-GmPUB13 U-box and Avr1d were loaded on a Superdex 200 gel-filtration column (GE Healthcare) and eluted in Superdex buffer (20 mM Tris [pH 8.0], 300 mM NaCl, 1 mM TCEP [tris(2-carboxyethyl)phosphine]) using the AKTA Explorer FPLC system (GE Healthcare). The protein was concentrated to 7.5 mg/mL.

Crystallization, Data Collection, and Structure Determination. Crystallization was conducted using the sitting-drop vapor diffusion method at 4 °C. Avr1d-GmPUB13 U-box yielded crystals with good diffraction quality in 12% wt/vol polyethylene glycol 20,000, 0.1 M BICINE pH 8.5 and 3% wt/vol dextran sulfate sodium salt. Before data collection, all crystals were soaked in the reservoir solution supplemented with 25% glycerol and flash cooled in liquid nitrogen. The diffraction data were collected at beamlines BL17U1 and BL19U1 at the Shanghai Synchrotron Radiation Facility and processed using the XDS program. A summary of the statistical methods used for data collection and analysis is provided in *SI Appendix*, Table S1. Phases were obtained experimentally with data from selenomethionine-substituted Avr1d-GmPUB13 U-box. The PHENIX software suite was used for initial model building. The final model was built by performing iterative manual model building with Coot and maximum likelihood refinement in PHENIX. Images and structural alignments were generated by using PyMOL.

Size Exclusion Chromatography (SEC) Assay. Purified GmPUB13(252-630) (roughly 40 μM) and Avr1d (roughly 40 μM) proteins were incubated at 4 °C for 1 h in the buffer containing 20 mM Tris [pH 8.0], 300 mM NaCl, 1 mM TCEP. GmPUB13(252-630), Avr1d, GmPUB13(252-630), and Avr1d, three samples were then injected onto a Superdex 200 gel-filtration column (GE) for analysis in line at a flow rate of 0.4 mL/min. The fractions (0.5 mL/fraction) were analyzed by SDS-PAGE electrophoresis and visualized by Coomassie brilliant blue staining. Mutant samples such as Avr1d^{F90A} were analyzed using the same method as described above.

Isothermal Titration Calorimetry. ITC-binding curves were measured by using a Microcal PEAQ-ITC instrument (Malvern). Purified proteins were transferred to buffer containing 20 mM Hepes pH 7.5, 100 mM NaCl, and 2 mM β-mercaptoethanol by 5 mL desalting column (GE). Titrations were performed at 20 °C. Titration of GmPUB13(252-630) in the cell was performed by sequential addition of Avr1d, GmE2, and Avr1d^{F90A} separately. Data were analyzed using Origin 7.0.

Data Availability. Protein structure data have been deposited in the RSCB Protein Data Bank (7C96).

ACKNOWLEDGMENTS. We thank the BL17U1 and BL19U1 of Shanghai Synchrotron Radiation Facility for support during crystallographic data collection. We thank W. Ma (University of California Riverside) for discussions and constructive suggestions. Research in the W.X. laboratory is supported by the Chinese Thousand Talents Plan and the Chinese Academy of Sciences. This research was supported by grants to Yuanchao Wang from the China National Funds for Innovative Research Groups (31721004), the Chinese Modern Agricultural Industry Technology System (CARS-004-PS14), the Key Program of the National Natural Science Foundation of China (31430073), and the Fundamental Research Funds for the Central Universities (KYXK202010). B.M.T. was supported by Oregon State University.

1. S. Hacquard, S. Spaepen, R. Garrido-Oter, P. Schulze-Lefert, Interplay between innate immunity and the plant microbiota. *Annu. Rev. Phytopathol.* **55**, 565–589 (2017).
2. Y. Ye, M. Rape, Building ubiquitin chains: E2 enzymes at work. *Nat. Rev. Mol. Cell Biol.* **10**, 755–764 (2009).
3. B. Zhou, L. Zeng, Conventional and unconventional ubiquitination in plant immunity. *Mol. Plant Pathol.* **18**, 1313–1330 (2017).
4. D. Chinchilla, Z. Bauer, M. Regenass, T. Boller, G. Felix, The *Arabidopsis* receptor kinase FLS2 binds flg22 and determines the specificity of flagellin perception. *Plant Cell* **18**, 465–476 (2006).
5. D. Lu *et al*., Direct ubiquitination of pattern recognition receptor FLS2 attenuates plant innate immunity. *Science* **332**, 1439–1442 (2011).
6. D. Liao *et al*., *Arabidopsis* E3 ubiquitin ligase PLANT U-BOX13 (PUB13) regulates chitin receptor LYSIN MOTIF RECEPTOR KINASE5 (LYK5) protein abundance. *New Phytol.* **214**, 1646–1656 (2017).
7. B. M. Tyler, *Phytophthora sojae*: Root rot pathogen of soybean and model oomycete. *Mol. Plant Pathol.* **8**, 1–8 (2007).
8. Q. Wang *et al*., Transcriptional programming and functional interactions within the *Phytophthora sojae* RXLR effector repertoire. *Plant Cell* **23**, 2064–2086 (2011).
9. W. Yin *et al*., The Phytophthora sojae Avr1d gene encodes an RxLR-dEER effector with presence and absence polymorphisms among pathogen strains. *Mol. Plant Microbe Interact.* **26**, 958–968 (2013).
10. X. Yang *et al*., Chemotaxis and oospore formation in *Phytophthora sojae* are controlled by G-protein-coupled receptors with a phosphatidylinositol phosphate kinase domain. *Mol. Microbiol.* **88**, 382–394 (2013).
11. L. S. Boutemy *et al*., Structures of Phytophthora RXLR effector proteins: A conserved but adaptable fold underpins functional diversity. *J. Biol. Chem.* **286**, 35834–35842 (2011).
12. Z. Xu *et al*., Interactions between the quality control ubiquitin ligase CHIP and ubiquitin conjugating enzymes. *BMC Struct. Biol.* **8**, 26 (2008).
13. S. Fan *et al*., GmWRKY31 and GmHDL56 enhances resistance to *Phytophthora sojae* by regulating Defense-Related gene expression in soybean. *Front. Plant Sci.* **8**, 781 (2017).
14. T. Xin *et al*., Genetic regulation of ethylene dosage for cucumber fruit elongation. *Plant Cell* **31**, 1063–1076 (2019).
15. W. J. Lyzenga, V. Sullivan, H. Liu, S. L. Stone, The kinase activity of Calcineurin B-like interacting protein kinase 26 (CIPK26) influences its own stability and that of the ABA-regulated ubiquitin ligase, Keep on going (KEG). *Front. Plant Sci.* **8**, 502 (2017).
16. P. de Bie, A. Ciechanover, Ubiquitination of E3 ligases: Self-regulation of the ubiquitin system via proteolytic and non-proteolytic mechanisms. *Cell Death Differ.* **18**, 1393–1402 (2011).
17. R. Ben-Saadon, D. Zaaroor, T. Ziv, A. Ciechanover, The polycomb protein Ring1B generates self atypical mixed ubiquitin chains required for its *in vitro* histone H2A ligase activity. *Mol. Cell* **24**, 701–711 (2006).
18. R. B. Abramovitch, R. Janjusevic, C. E. Stebbins, G. B. Martin, Type III effector AvrPtoB requires intrinsic E3 ubiquitin ligase activity to suppress plant cell death and immunity. *Proc. Natl. Acad. Sci. U.S.A.* **103**, 2851–2856 (2006).
19. J. Dong *et al*., Crystal structure of the complex between *Pseudomonas* effector AvrPtoB and the tomato Pto kinase reveals both a shared and a unique interface compared with AvrPto-Pto. *Plant Cell* **21**, 1846–1859 (2009).
20. J. Qin *et al*., The *Xanthomonas* effector XopK harbours E3 ubiquitin-ligase activity that is required for virulence. *New Phytol.* **220**, 219–231 (2018).
21. C. H. Park *et al*., The *Magnaporthe oryzae* effector AvrPiz-t targets the RING E3 ubiquitin ligase APIP6 to suppress pathogen-associated molecular pattern-triggered immunity in rice. *Plant Cell* **24**, 4748–4762 (2012).
22. L. Yang *et al*., Potato NPH3/RPT2-like protein StNRL1, targeted by a *Phytophthora infestans* RXLR effector, is a susceptibility factor. *Plant Physiol.* **171**, 645–657 (2016).
23. Q. He *et al*., Plant pathogen effector utilizes host susceptibility factor NRL1 to degrade the immune regulator SWAP70. *Proc. Natl. Acad. Sci. U.S.A.* **115**, E7834–E7843 (2018).
24. J. I. B. Bos *et al*., *Phytophthora infestans* effector AVR3a is essential for virulence and manipulates plant immunity by stabilizing host E3 ligase CMPG1. *Proc. Natl. Acad. Sci. U.S.A.* **107**, 9909–9914 (2010).
25. C. Hua *et al*., A *Phytophthora sojae* G-protein α subunit is involved in chemotaxis to soybean isoflavones. *Eukaryot. Cell* **7**, 2133–2140 (2008).
26. Y. Fang *et al*., Efficient genome editing in the Oomycete Phytophthora sojae using CRISPR/Cas9. *Curr. Protoc. Microbiol.* **44**, 21A.1.1–21A.1.26 (2017).
27. S. Subramanian, M. Y. Graham, O. Yu, T. L. Graham, RNA interference of soybean isoflavone synthase genes leads to silencing in tissues distal to the transformation site and to enhanced susceptibility to *Phytophthora sojae*. *Plant Physiol.* **137**, 1345–1353 (2005).
28. Z. Ma *et al*., A paralogous decoy protects *Phytophthora sojae* apoplastic effector PsXEG1 from a host inhibitor. *Science* **355**, 710–714 (2017).
29. Q. Zhao, L. Liu, Q. Xie, "In vitro protein ubiquitination assay" in *Plant Signaling Networks: Methods and Protocols*, Z. Wang, Z. Yang, Eds. (Springer, 2012), pp. 163–172.